Therapeutic Potential of AntagomiR-23b for Treating Myotonic Dystrophy

Estefanía Cerro-Herreros,[1,2,3] Irene González-Martínez,[1,2,3] Nerea Moreno-Cervera,[1,2,3] Sarah Overby,[1,2,3] Manuel Pérez-Alonso,[1,2,3] Beatriz Llamusí,[1,2,3] and Rubén Artero[1,2,3]

[1]Interdisciplinary Research Structure for Biotechnology and Biomedicine (ERI BIOTECMED), Universidad de Valencia, 46100 Valencia, Spain; [2]Translational Genomics Group, Incliva Health Research Institute, 46010 Valencia, Spain; [3]Joint Unit Incliva-CIPF, Valencia, Spain

Myotonic dystrophy type 1 (DM1) is a chronically debilitating, rare genetic disease that originates from an expansion of a non-coding CTG repeat in the dystrophia myotonica protein kinase (*DMPK*) gene. The expansion becomes pathogenic when *DMPK* transcripts contain 50 or more repetitions due to the sequestration of the muscleblind-like (MBNL) family of proteins. Depletion of MBNLs causes alterations in splicing patterns in transcripts that contribute to clinical symptoms such as myotonia and muscle weakness and wasting. We previously found that microRNA (miR)-23b directly regulates MBNL1 in DM1 myoblasts and mice and that antisense technology ("antagomiRs") blocking this microRNA (miRNA) boosts MBNL1 protein levels. Here, we show the therapeutic effect over time in response to administration of antagomiR-23b as a treatment in human skeletal actin long repeat (HSA^LR) mice. Subcutaneous administration of antagomiR-23b upregulated the expression of MBNL1 protein and rescued splicing alterations, grip strength, and myotonia in a dose-dependent manner with long-lasting effects. Additionally, the effects of the treatment on grip strength and myotonia were still slightly notable after 45 days. The pharmacokinetic data obtained provide further evidence that miR-23b could be a valid therapeutic target for DM1.

INTRODUCTION

Myotonic dystrophy type 1 (DM1) is a rare genetic disease with no current effective treatment. DM1 is associated with a substantial disease burden resulting in impairment across many different patient systems and tissues. Muscle weakness and fatigue constitute the two most common disease manifestations, reported by 93% and 90% of patients, respectively, followed by muscle locking (73%).[1] Other phenotypes include cardiac dysfunctions, cataracts, insulin resistance, and intellectual disability (OMIM; MIM: 160900). The disease is based on CTG repeat expansions occurring in the dystrophia myotonica protein kinase (*DMPK*) gene, which are transcribed into pathogenic mRNAs. The CUG repeats bind with high affinity to the muscleblind-like (MBNL) family of proteins, thereby inhibiting their normal function.[2,3] In skeletal muscle and brain, MBNL1 and MBNL2, respectively, are preferentially expressed, whereas MBNL3 is expressed primarily during embryonic development and adult tissue regeneration.[4] MBNL1 proteins are responsible for the regulation of splicing of several transcripts, specifically by causing a shift from fetal to adult splicing patterns,[5–7] and act antagonistically to CUGBP Elav-like family member 1 (CELF) proteins in splice regulation, which are found upregulated in DM1.[8,9] Consequently, transcripts, such as *CLCN1*, *INSR*, *BIN1*, and *DMD*, inappropriately take on a fetal splicing pattern, which leads to clinical symptoms.[10–14] Indeed, the correction of erroneous *Clcn1* alternative splicing in mouse models of DM eliminates chloride channelopathy and myotonia.[12] MBNL proteins control RNA metabolism in additional ways, including fetal-to-adult polyadenylation patterns, stability, differential localization of mRNAs, and miRNA biogenesis.[15–18]

The depletion of MBNL protein function has been shown to be a critical factor in the course of the disease. In loss-of-function experiments, *Mbnl1* knockout mice and compound loss of *Mbnl1* and *Mbnl2* recapitulate several clinical symptoms for DM1, including myotonia, mis-splicing, reduced lifespan, and progressive skeletal muscle weakness.[19,20] *Mbnl1* knockout in mice also reflected the various cardiac dysfunctions and embryonic splice isoforms seen in human DM1 patients.[21] Indeed, MBNL1 loss of function accounts for more than 80% of mis-splicing events and nearly 70% of expression defects.[22] In complementary gain-of-function experiments, upregulation of Mbnl1, using a recombinant adeno-associated viral vector in a murine model that expresses 250 CTG repeats in the context of human skeletal actin long repeat (HSA^LR mice), rescued myotonia and mis-splicing of *Clcn1*, *Zasp*, *Serca1*, and *Tnnt3*.[23] Likewise, overexpression of Muscleblind in the CUG repeats *Drosophila* model rescued eye phenotypes and heart and muscle histopathology, as well as reduced nuclear foci.[24–26] Muscleblind overexpression also rescued muscle atrophy and excessive autophagy levels in an inducible fly model,[27] and autophagy was reduced after treatment with Muscleblind-increasing chloroquine treatment in the same model.[28] MBNL1 upregulation in DM1 mice and patient-derived fibroblasts is well tolerated and rescues several symptoms, such as myotonia and mis-splicing events, as well as the reduction of foci

formation.[29–31] Finally, genetic variations in the promoter of *MBNL1* have been shown to correlate with disease severity, further implicating *MBNL1* in DM1.[32] Thus, DM1 is likely treatable because limited function of MBNL proteins can be compensated by enhanced expression of their normal endogenous genes.

The sequestration of MBNL1 in the *DMPK* repeats is not the only factor inhibiting its function. MicroRNAs (miRNAs) are regulators of the expression of mRNA transcripts and can have dozens of targets. By complementary binding to the 3′ UTR of mRNAs, miRNAs guide the RNA-induced silencing complex (RISC) and signal them for translational repression and decay.[33] miRNAs are known to play a critical role in the mechanisms of DM1,[34] especially once it was found that using miRNA sponges in DM1 *Drosophila* de-represses *muscleblind* and rescues muscle atrophy, improves lifespan, and reverses splicing events.[35] In human cells, the expression of microRNA-23b-3p (hereafter referred to as miR-23b) is of importance in DM1, because it has been shown to regulate *MBNL1* and *-2* transcripts directly by luciferase reporter assay, and the silencing of this miRNA by use of antisense oligonucleotides, termed antagomiRs, induced a statistically significant improvement of pathological symptoms in DM1 cells and mice.[36] In this study, we show the therapeutic response to the cholesterol-conjugated antagomiR-23b administration in dosage by subcutaneous and intravenous routes and washout time in an HSA[LR] mice model. By observing and quantifying the molecular response to drug administration, we conclude that miR-23b suppression by the use of antagomiRs is a viable treatment for DM1 in precise correspondence with miR-23b as a possible therapeutic target.

RESULTS
Therapeutic Effects of AntagomiRs Are Similar Using Subcutaneous or Intravenous Administration Routes
We have recently demonstrated that an antagomiR that reduces the activity of miR-23b in mammalian DM1 models, including patient cells and HSA[LR] mice, can rescue DM1-like phenotypes.[36] In this previous study, we observed that miR-23b can bind directly to the 3′ UTR of *MBNL1*. We also observed that a single subcutaneous injection of the antagomiR against miR-23b at 12.5 mg/kg obtained significant rescue of Mbnl1 levels, mis-splicing, histological phenotypes, myotonia, and grip strength in HSA[LR] mice. In order to investigate whether the use of another route of administration could improve the efficacy of the antagomiR treatment in muscles, we compared the phenotypes of HSA[LR] mice treated with antagomiR-23b or antagomiR-scramble (SC) as a control for the chemistry of the antisense oligonucleotide at a concentration of 12.5 mg/kg by subcutaneous and tail-vein injection (intravenously [i.v.]). 4 days after injection, the animals were sacrificed, and the quadriceps (QD) and gastrocnemius (GT) muscles of the hind limbs were dissected to study the molecular effects of the treatments (Figure 1A).

We observed that antagomiR-23b, injected using intravenous administration, was only slightly more efficient in reducing miR-23b levels (Figure S1) and produced a significantly higher increase of *Mbnl1* transcripts (Figures 1B and 1C), but in correlation with the miRNA

levels, there was no significant difference between the Mbnl1 protein levels obtained with subcutaneous and the intravenous routes (Figures 1D–1G). Subsequent to this ELISA test, we verified the existence of both the nuclear and cytoplasmic fractions of Mbnl1 in the samples of both muscles extracted with PBS for the subcutaneous administration test. To do this, we carried out a western blot experiment in which we detected histone H3, a well-known nuclear protein; glyceraldehyde 3-phosphate dehydrogenase (Gapdh) for the cytoplasmic fraction; and Mbnl1, our study protein. As observed in Figure S2, in all of the western blot lanes, the presence of histone H3, Gapdh, and Mbnl1 is observed. This indicates that, despite extracting the protein with PBS, both nuclear and cytoplasmic phases of our protein are present in the extraction. The improvement of force, measured as percentage of normal force (PNF), and myotonia, was also similar using both routes (Figures 1H and 1I). Importantly, blood serum biochemistry, measured in total blood extracted before sacrifice, showed that the intravenous administration produced more alterations in comparison to the subcutaneous treatment and normalized to PBS (Table S1, tab A). Specifically, the amylase, alanine aminotransferase (ALT), and bile acid levels were significantly increased compared to the DM1 mice injected subcutaneously with antagomiR-23b, which could be biomarkers of pancreas and liver-related alterations. The SC also showed alterations in lipase after intravenous injection. However, although increased, the levels achieved were not enough to be considered clinically relevant, according to previous reports.[37] Weight was evaluated before the treatment and again before sacrifice. Unaltered weight and visual necropsy confirmed that there were no relevant toxic effects in the treated mice. Analyzing together the white blood cell differential count of mice administered with antagomiR-23b with both types of administration, significant differences were found (*p = 0.0047), indicating that intravenous administration does produce changes, which supports our decision to administer subcutaneously. In the case of SC, no significant changes are seen. This is observed in the dendrograms of Table S1, tab B, where it is shown how mice treated with intravenously administered antagomiR-23b show a tendency to form a cluster, and those treated subcutaneously form another. This indicates that there is a significant difference between both routes of administration. Since there was not a significant difference between the delivery routes in Mbnl1 protein and functional improvement and also because of the biochemical blood and serum alterations seen in intravenous injection, the subcutaneous injection was chosen for the rest of drug administrations in this study, as it is less invasive and would be preferable in cases of administration to patients as a chronic treatment.

Effects of AntagomiR-23b after Subcutaneous Injection Depend on Dosage
In order to define the dose range in which antagomiR showed therapeutic effects, we studied the effects of subcutaneous injection of antagomiR-23b or -SC as a negative control at a dose approximately 4 times lower (3 mg/kg) and 4 times higher (40 mg/kg) than the previously used dose of 12.5 mg/kg. 4 days after injection, the animals were sacrificed, and the QD and GT muscles of the hindlimbs were dissected for molecular study (Figure 2A). The results showed a
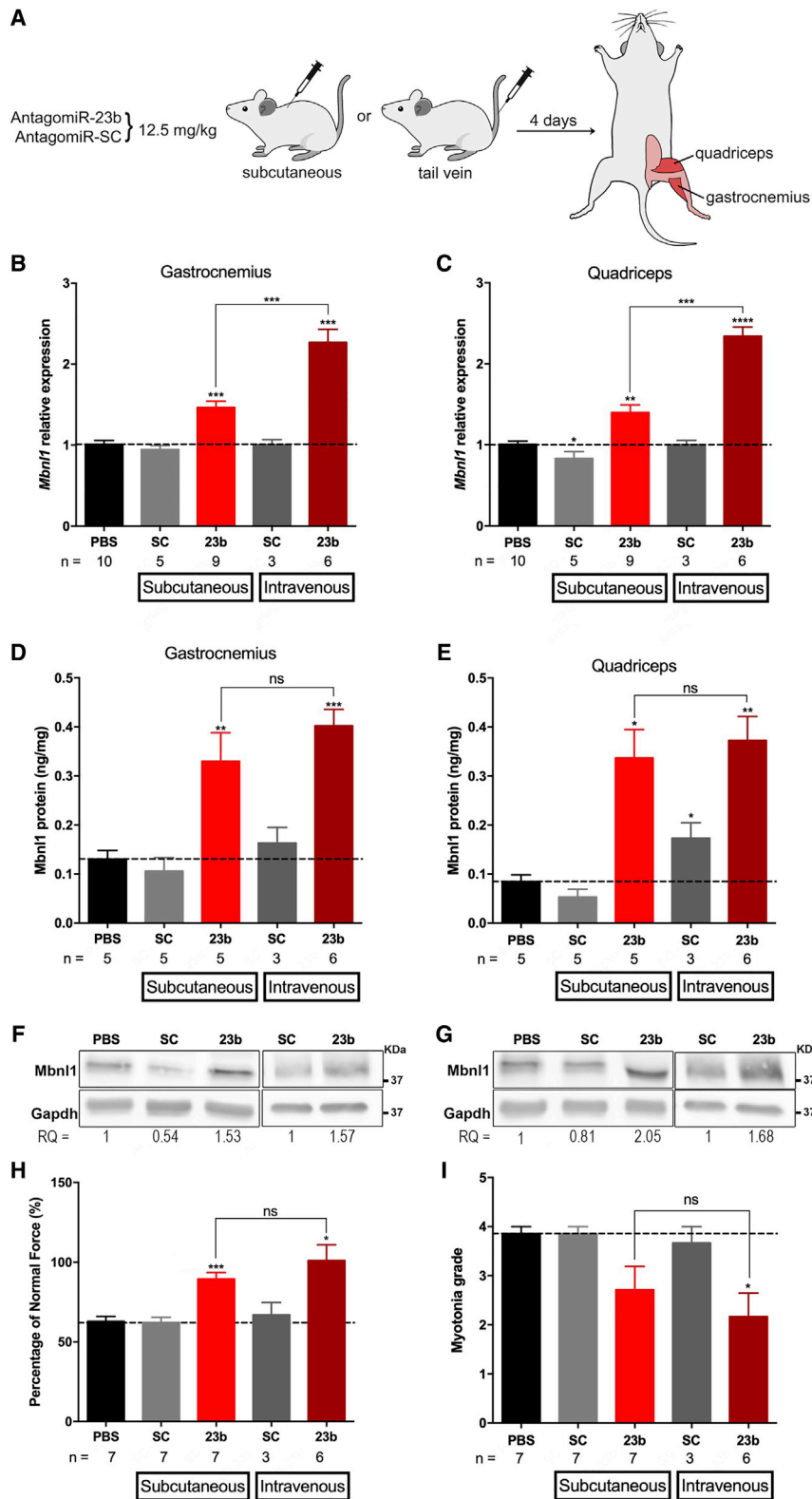
A

Figure 1. Comparative Study between Subcutaneous and Intravenous Delivery of AntagomiRs in Mice

(A) Administration protocol for subcutaneous and intravenous injections of antagomiR-23b (23b) and antagomiR-SC (SC). All administrations were performed at a concentration of 12.5 mg/kg. (B and C) *Mbnl1* relative transcript expression was quantified in gastrocnemius (B) and quadriceps (C) muscles using *Gapdh* as the endogenous control. (D and E) Mbnl1 relative protein expression was quantified by ELISA in gastrocnemius (D) and quadriceps (E) muscles and was normalized to total protein. (F and G) Western blots from pooled samples were also relatively quantified (RQ) in support of the ELISA results. Mbnl1 relative protein level was measured from gastrocnemius (F) and quadriceps (G) muscles and normalized to Gapdh. (H and I) Before sacrifice, mice were evaluated for grip strength (H), represented as percentage of normal force (PNF), and myotonia grade (I). Statistical comparisons shown were all performed against PBS-treated HSA[LR] mice data (black dashed lines) via Student's t-test. Additionally, results between mice treated with antagomiR-23b subcutaneous or intravenously were compared in all panels. p values: ns = not significant, *p < 0.05, **p < 0.01, and ***p < 0.001. Error bars = standard error of the mean (SEM).
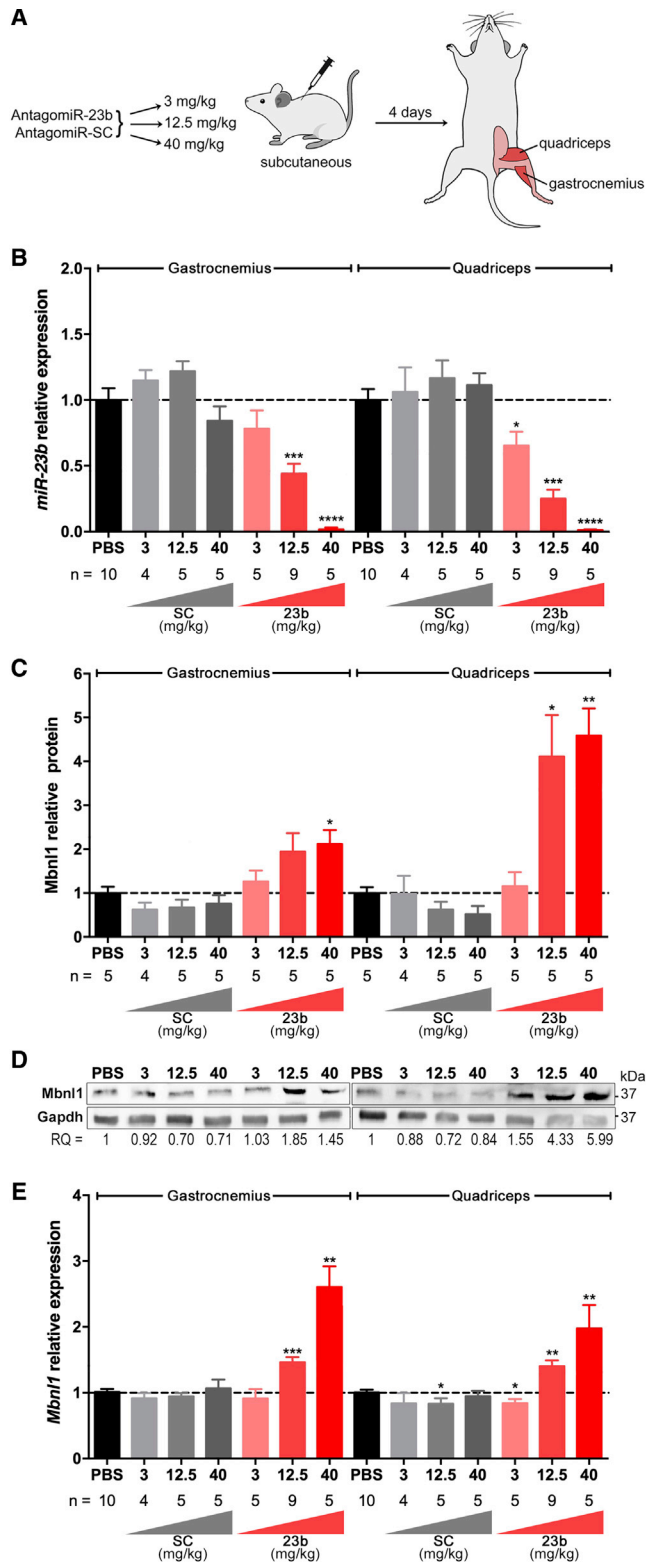
B Gastrocnemius

C Quadriceps

D Gastrocnemius

E Quadriceps

F

G

H

I

Figure 2. Dose-Response Study of Gene Expression and Protein after Treatment with AntagomiRs

(A) Administration protocol for a dose-response study was performed at 3 different concentrations: 3 mg/kg, 12.5 mg/kg, and 40 mg/kg by subcutaneous injection of PBS, antagomiR-23b (23b), and antagomiR-SC (SC). After 4 days, gastrocnemius and quadriceps muscles were dissected for analysis. (B) miR-23b relative expression was quantified from gastrocnemius and quadriceps muscles relative to $U1$ and $U6$ snRNA endogenous controls. (C) Mbnl1 relative protein level was measured from gastrocnemius and quadriceps muscles using ELISA and normalized to total protein. (D) Representative western blots from pooled samples were also RQ in support of the ELISA results. Mbnl1 relative protein level was measured from gastrocnemius and quadriceps muscles and normalized to Gapdh. (E) $Mbnl1$ relative transcript expression was also assessed from gastrocnemius and quadriceps muscles relative to $Gapdh$ endogenous control. Statistical comparisons shown were all performed against PBS-treated HSA[LR] mice data (black dashed lines) via Student's t-test. p values: *p < 0.05, **p < 0.01, and ***p < 0.001. Error bars = SEM.

dose-dependent decrease in miR-23b levels in both muscles (Figure 2B), only when antagomiR-23b and not SC was administered, which was concurrent to an increase of Mbnl1 at mRNA and protein levels (Figures 2C–2E). ELISA results for protein measurements were confirmed with western blot (Figure 2D). AntagomiR-23b at 3 mg/kg produced a slight but significant reduction of miR-23b in QD, which was not able to increase Mbnl1 protein or mRNA levels. Of note, reductions of more than 50% of miR-23b, obtained with the 12.5 mg/kg dose, produced a significant effect on Mbnl1 at both mRNA and protein levels. The 40-mg/kg dose achieved reductions in the miRNA levels of more than 90% and produced an important increase in the levels of $Mbnl1$ mRNA compared to the treatment with 12.5 mg/kg. This difference was not so prominent at the level of protein. Importantly, the administration of antagomiR-SC had no effect on the miRNAs or the Mbnl1 levels even at the highest concentration. In order to verify the direct effect of the antagomiR-23 on Mbnl1 and to rule out other possible effects of the silencing of the miRNA within the context of the disease, the levels of the HSA transgene that HSA[LR] mice carry were measured by qRT-PCR. The qRT-PCR results revealed that treatment with antagomiRs-SC and -23b compared to PBS did not exert any effect on the HSA transgene in any of the study situations (Figure S3), ruling out a possible effect of these oligonucleotides at this level.

In parallel with the levels of Mbnl1 protein measured, Mbnl1-dependent splicing rescue was also observed in a dose-response manner for $Nfix$ and $Clcn1$ transcripts, either in GT or QD muscles (Figures 3A–3D). There was a reduction in the inclusion of exon 7 and exon 7a, respectively. Representative electrophoresis gels for $Nfix$ and $Clcn1$ can be visualized in Figure S4. Recovery of $Clcn1$ splicing was concomitant to an improvement of myotonia levels after injection with antagomiR-23b (Figure 3E), which is in agreement with previous studies.[12] Grip strength increased in a dose-dependent manner, as well after treatment (Figure 3F). Of note, in both myotonia and grip-strength tests, we observed no difference between the results of mice treated at the concentration of 12.5 mg/kg or 40 mg/kg, which correlated with the levels of Mbnl1 protein detected.
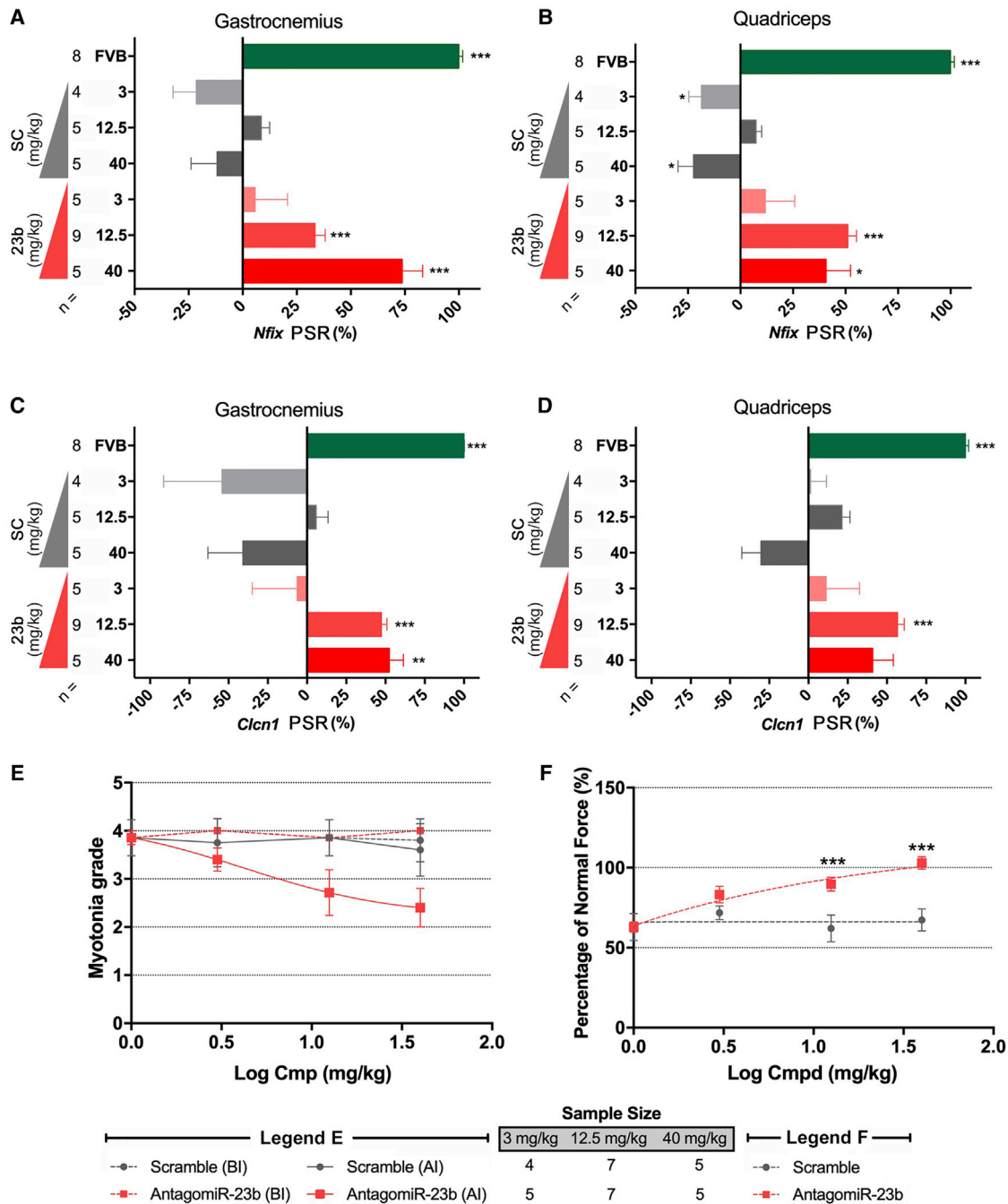
Figure 3. Dose-Response Study of Splicing, Myotonia, and Force after Treatment with AntagomiRs

(A–D) After treatment with PBS, antagomiR-23b (23b) and antagomiR-SC (SC) percent splicing recovery was calculated for *Nfix* (A and B), as well as *Clcn1* (C and D) in gastrocnemius (A and C) and quadriceps (B and D) muscles. (E and F) Myotonia (E) and grip strength (F) were analyzed before injection (BI) and 4 days after injection (AI). (A–D and F) All statistical comparisons were performed against the data obtained in PBS-treated HSA^{LR} mice via Student's t-test. p values: *p < 0.05, **p < 0.01, and ***p < 0.001. Error bars = SEM.

The component's analysis of serum biochemistry studies revealed that neither antagomiR-SC nor antagomiR-23b treatments caused significant alterations in comparison to PBS treatment, arguing against a specific effect of the miRNA reduction in the immune system activation (Table S1, tab C). Importantly, antagomiR-23b had no other relevant effects in the levels of the different tissue-damage biomarker
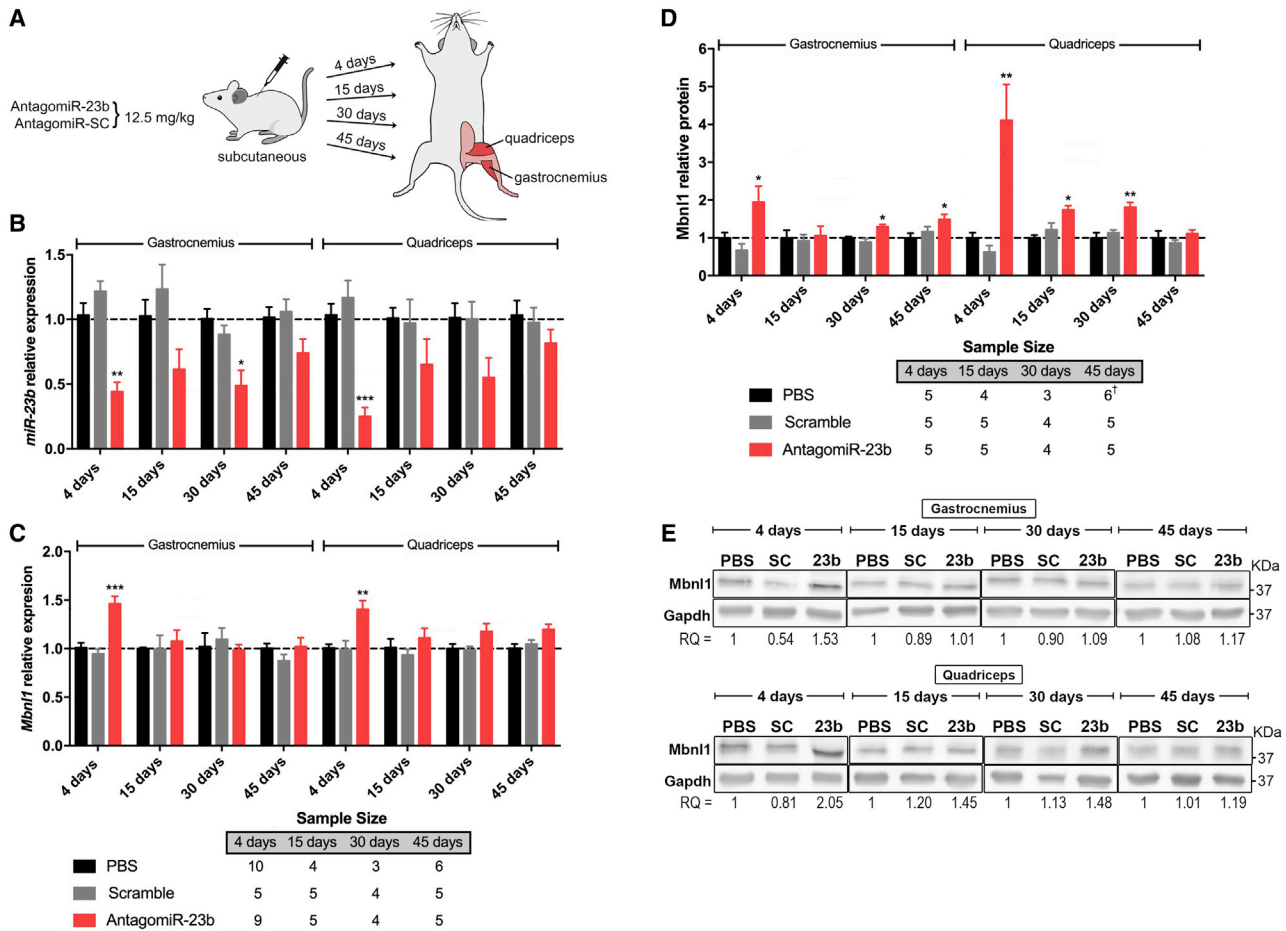
Figure 4. Time-Response Study of Gene Expression and Protein after Treatment with AntagomiRs

(A) Administration protocol for time-response study was performed at the concentration of 12.5 mg/kg via subcutaneous injection of PBS, antagomiR-23b (23b), and antagomiR-SC (SC). Mice were sacrificed 4, 15, 30, and 45 days after injection, and quadriceps and gastrocnemius muscles were dissected. (B) miR-23b relative expression was quantified from gastrocnemius and quadriceps muscles relative to *U1* and *U6* snRNA endogenous controls. (C) *Mbnl1* relative transcript expression was also assessed from gastrocnemius and quadriceps muscles relative to *Gapdh* endogenous control. (D) Mbnl1 relative protein level was measured in ELISA from gastrocnemius and quadriceps muscles and normalized to total protein. †Quadriceps PBS 45 days, n = 5. (E) Western blots from pooled samples were also quantified in support of the ELISA results. Mbnl1 relative protein level was measured from gastrocnemius and quadriceps muscles and normalized to Gapdh. A legend for graph bar colors can be found at the bottom left of the figure. All statistical comparisons were performed against the data obtained in PBS-treated HSA^{LR} mice (black dashed lines) via Student's t-test. p values: *p < 0.05, **p < 0.01, and ***p < 0.001. Error bars = SEM.

analyzed and did not affect the weight of the animals or cause any other macroscopic alteration that could be detected in the necropsy at all of the dosages tested. Although the administration of the antagomiR at high doses has no effect on blood biochemistry and weight, the statistical analysis with ANOVA and Kruskal-Wallis revealed statistically significant changes between Friend leukemia virus B (FVB) and HSA^{LR} mice treated with PBS, SC, and antagomiR-23 for the levels of urea, lipase, and weight. This is novel data and indicates that these are changes that are normally present between healthy mice and mice modeling the disease. As for the white blood cell differential count, there were no significant differences between the groups (p = 0.0665), which means that there are no alterations in blood composition either by treatment or by dose. This can be

observed in the dendrogram (Table S1, tab D), since the treated mice are not grouped into clusters. Overall, it seems that there are not relevant changes in blood biochemistry parameters depending on concentration.

One Single Injection of AntagomiR-23b Produces Long-Lasting Phenotypical Alterations

To define the period of effective treatment of DM1 phenotypes, we injected the antagomiR-23b or -SC at 12.5 mg/kg through subcutaneous injection and sacrificed the animals at different times postinjection (4, 15, 30, and 45 days) (Figure 4A). The GT and QD muscles from the hindlimbs were dissected after sacrifice, and total RNA and protein were quantified for levels of target miRNA, *Mbnl1*
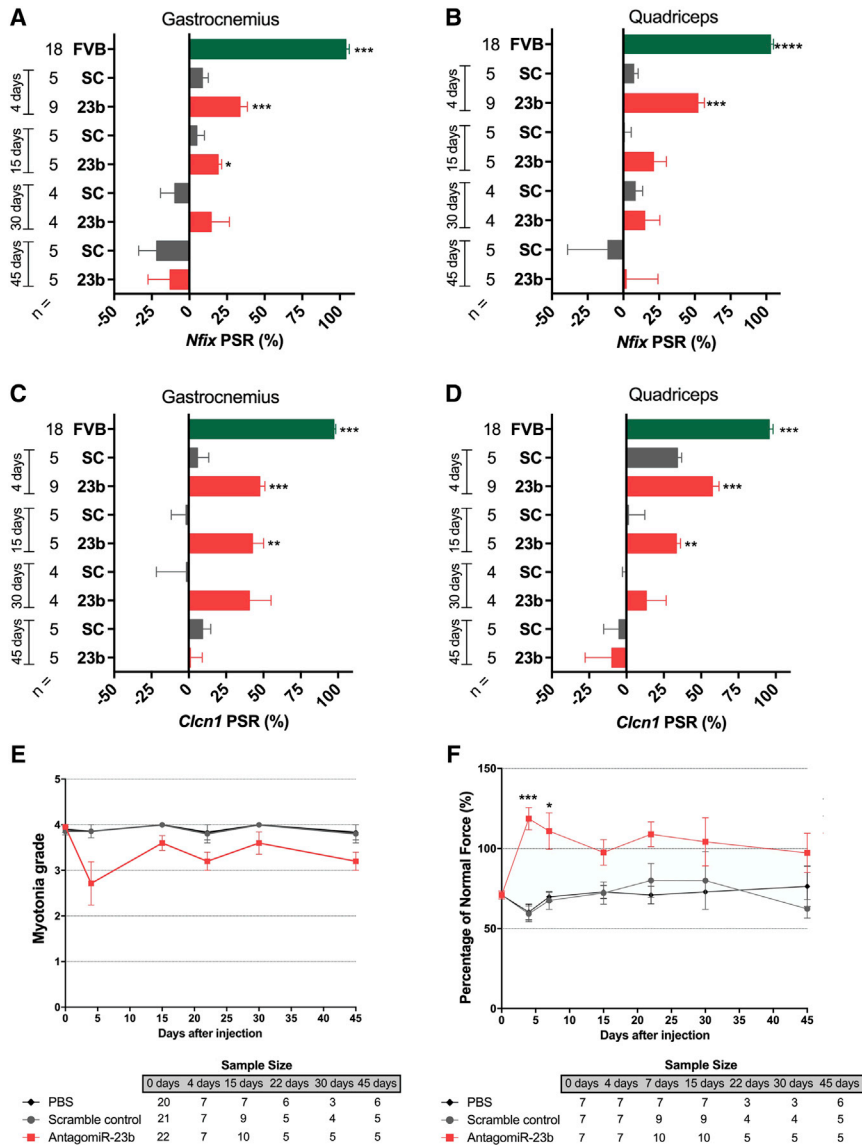
Figure 5. Time-Response Study of Splicing, Myotonia, and Force after Treatment with AntagomiRs

(A–D) After treatment with PBS, antagomiR-23b (23b), and antagomiR-SC (SC), percent splicing recovery was calculated for *Nfix* (A and B), as well as *Clcn1* (C and D) in gastrocnemius (A and C) and quadriceps (B and D) muscles. (E and F) Myotonia (E) and grip strength (F) were analyzed before injection, at intermediate time points, and before the sacrifice. (A–D and F) All statistical comparisons were performed against the data obtained in PBS-treated HSA^LR mice via Student's t-test. p values: *p < 0.05, **p < 0.01, and ***p < 0.001. Error bars = SEM.

The sustained effect of treatment with antagomiR-23b was also detected in the functional studies. Before sacrifice, mice were evaluated for grip strength and myotonia (Figures 5E and 5F). Although the greatest effect of rescue was again observed 4 days after injection, a reduction in myotonia and an increase in grip strength continued to be evident even 45 days after the injection. The component's analysis of blood serum biochemistry studies and white blood cell differential counts showed no significant alterations caused by antagomiR-23b treatment at the different time-point studies in comparison to PBS treatment, except for amylase (Table S1, tab E). Visual necropsy and weight control showed no other significant alterations in the treated animals. There are significant differences in the weight in FVB compared to the PBS. For amylase, there is a significant difference between 23b and FVB in comparison to PBS (p = 0.027) compared to the rest of treatments, which means that we managed to reverse the levels of amylase from mice treated to those of FVB. As for the white blood differential count, there are no significant differences between the groups (p = 0.4856), which means that there are no alterations in blood composition either by treatment or by time. This can be observed in the dendrogram (Table S1, tab F), since the treated mice are not grouped into clusters. These results suggest that although the effects of antagomiRs on Mbnl1 levels and functional improvement are maintained in time, they do not have any delayed effect on blood biochemistry or tissue damage.

Effects of AntagomiR-23b after Subcutaneous Injection in the Mbnl1 Distribution and Foci in Muscle Fibers

From the previous experiments, we have been able to establish the subcutaneous route as a suitable administration mode for the antagomiR-23b. In the dose-response and time-response experiments, we see a plateau effect of Mbnl1 growth and miR-23b decline between the concentrations of 12.5 and 40 mg/kg and that the duration
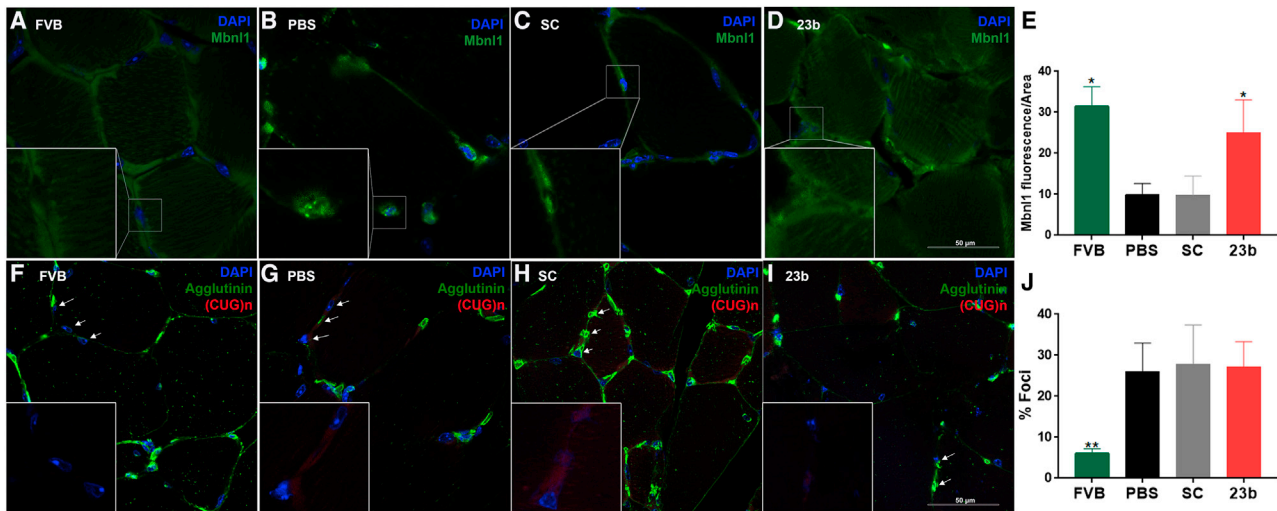
transcripts, and protein and the effect on Mbnl1-dependent splicing events. With regard to molecular changes, the highest therapeutic effects were observed 4 days after injection (Figure 4). However, there was a clear tendency to maintain reduced levels of miRNA and increased levels of Mbnl1 protein over time. A mild but significant overexpression of Mbnl1 protein levels was detected even 30 days in QD after a single injection and 45 days in GT after a single injection (Figures 4D and 4E). Of note, these levels of protein were enough to exert an effect on Mbnl1-dependent splicing events up to 15 days postinjection (Figure 5). Significant splice recovery was also seen for up to 15 days in transcripts for *Clcn1* in GT and QD samples and in *Nfix* for GT samples. There was a reduction in the inclusion of exon 7 in *Nfix* and exon 7a in *Clcn1*, respectively. Representative electrophoresis gels of *Nfix* and *Clcn1* splicing can be visualized in Figure S5.

Figure 6. Increase of Mbnl1 upon Silencing of miR-23b in Mice Muscle

(A–D) Representative confocal images of Mbnl1 (green) staining in healthy mice (FVB) and HSA[LR] mice after subcutaneous injection with antagomiR-23b (23b), antagomiR-SC (SC), and PBS. Nuclei were counterstained with DAPI (blue). In HSA[LR] quadriceps, endogenous Mbnl1 was in nuclear aggregates (green puncta), and the total amount of protein was reduced compared to FVB muscles (A). In contrast, HSA[LR] quadriceps muscle treated with antagomiR-23b showed a robust increase in cytoplasmic and nuclear Mbnl1 levels in the fibers (D) compared to HSA[LR] controls antagomiR-SC (C) and PBS (B). (E) Quantitation of Mbnl1 signal from Mbnl1 IF. (F–I) Representative fluorescence of fluorescence in situ hybridization (FISH) images showing (CUG)n RNA foci (red) performed with cryosections from the quadriceps of untreated FVB (F) and treated HSA[LR] mice with antagomiR-23b (I), antagomiR-SC (H), and PBS (G). Green, wheat germ agglutinin staining (green) to highlight individual myofibers; blue, DAPI staining of nuclei. (J) Quantitation of the percentage of foci from FISH images. For Mbnl1 IF and foci quantification, a total of $8 \times 40 \times$ fields from each mice was counted: n = 4 with FVB, PBS, and antagomiR-23; n = 5 with antagomiR-SC. Scale bars, 50 μm. All cryosections were 10 μm thick, and images were compiled from multiple projections in z-plane stacks. p values: *p < 0.05, **p < 0.01, and ***p < 0.001. Error bars = SEM.

of this effect is between 4 and 15 days. Therefore, we selected subcutaneous injection, a 12.5-mg/kg dose, and a time of 4 days to carry out two important tests to better understand the mechanism of action of the antagomiR-23b. In the first of the tests, we used immunofluorescence (IF) to analyze the location of the Mbnl1 protein in the muscle fibers of HSA[LR] mice treated with PBS and antagomiR-SC and -23b. FVB mice were used as control of a normal Mbnl1 distribution. With support of the previous experiments, the increase in Mbnl1 protein detected in western blotting and ELISA with the antagomiR-23b was also detected by IF (Figure 6D). With the consideration that the Mbnl1 protein is sequestered in ribonuclear foci in HSA[LR] mice, treatment with the antagomiR-23b compared to PBS or SC produced a significant increase in Mbnl1 expression and restored its distribution at the nucleus and cytoplasm level in muscle fibers. This distribution was similar to that observed in healthy FVB mice (Figures 6A–6E). This increase in Mbnl1 that we see in the muscle at the nuclear level is consistent with the splicing rescue shown previously at the 12.5-mg/kg dose. Since there is a complex balance among MBNL proteins, their sequence, and the formation of the characteristic ribonuclear foci of DM1 itself,[38] a possible adverse effect to the increase in Mbnl1 could be a greater formation of foci. To test this hypothesis specifically, we quantified these foci in QD of mice treated with antagomiRs and PBS and discovered that they remained unchanged (Figures 6G–6J). In FVB, the existence of foci was practically nonexistent, as expected (Figure 6F).

DISCUSSION

A little-explored therapeutic strategy for DM1 is in the concept of therapeutic gene modulation, which seeks to increase or decrease the endogenous expression of a gene to alleviate a certain pathological state. Paradigmatic examples are the inhibition of estrogen receptors by antagonists in breast cancer or pharmacologically potentiating the expression of utrophin, a gene that is normally only expressed in the fetus, to compensate for the lack of dystrophin in Duchenne muscular dystrophy.[39] For DM1, the strategy intends to enhance the endogenous expression of MBNLs, for which activity is limited in the disease by sequestration to expansions, which, as described above, cause symptoms such as atrophy, myotonia, and heart disease. In this work, we provide further evidence that miR-23b could be a valid therapeutic target for DM1, which we have previously shown to repress MBNL1 and -2 in natural conditions and in which blockage increases the levels of both proteins in model cells and DM1 mice.[36]

We first show that there is a clear correlation between doses of antagomiR-23b and the degree of repression of miR-23b and an increase in the levels of *Mbnl1* transcripts in mice, which does not occur in mice that are administered a control with the same chemistry but SC sequence. This dose-response is no longer observed in levels of Mbnl1 proteins and functional muscle measurements, such as myotonia and muscle strength, where the difference between doses of 12.5 mg/kg and 40 mg/kg is relatively small. This may be due to

a certain plateau effect where more repression of miR-23b results in discrete increases—which have only small, additional improvements at the functional level—at the level of the Mbnl1 protein. We consistently saw an increase in the level of *Mbnl1* transcripts. Curiously, this increase was not proportional in Mbnl1 protein levels even at the highest dose. Perhaps low levels of miR-23b have little impact on MBNL1 transcript stability but still manage to keep transcripts from being translated into protein, which can be expected from miR-NAs that typically act within a precise margin. This may also be due to mRNA accumulation as P-bodies or stress granules, resulting in the transcript not being translated into protein.[40,41] Another explanation can be due to alternative splicing, which can change the subcellular localization of mRNAs and potentially contribute to the lack of MBNL1 protein being made. For example, in order for integrin α-3 transcripts to be translated, they must be located in focal adhesions, a process regulated by MBNL2.[42] That being said, the medium dosage of 12.5 mg/kg showed remarkable rescue of *Mbnl1* transcripts. However, at the 40-mg/kg dose, the transcribed levels of Mbnl1 in mouse muscle exceeded 2 to 2.5 times the level of endogenous expression in FVB mice, according to the levels observed in other experiments where the level of expression of *Mbnl1* mRNA between HSA[LR] mice treated with PBS and FVB is similar.[28] Likewise, the 12.5-mg/kg dosage also shows a healthy rescue of Mbnl1 protein levels and distribution, mis-splicing, myotonia, and muscle weakness. These results emphasize that antagomiR-23b can be fine-tuned to an effective and nontoxic concentration.

The results from the time-response study were particularly promising after observing rescue effects well after 4 days of treatment. The antagomiR showed efficient entry into the mice muscle cells evidenced by the significant biological and physiological effects (i.e., myotonia and grip-strength tests). Interestingly, these effects, although statistically non-significant, were still seen slightly, even after 45 days of the initial injection. It is true that the effect of the antagomiRs strongly decreases after 4 days, but over time, the decrease is much slower. Indeed, the effect seen at 45 days was similar to the amount of rescue observed at the minimal therapeutic dose of 3 mg/kg. It should be noted as well that the administration of this 12.5-mg/kg dose had no effect on the HSA transgene nor on the percentage of foci, thus ruling out the possible off-target effects that antagomiR-23b could have at this level.

It is encouraging to see that reducing the activity of a miRNA by only a small amount can have relevant therapeutic effects. Indeed, a reduction of around 50% in miR-23b was sufficient for the increase in Mbnl1 levels, which led to significant splicing and muscle-function improvements downstream. In fact, a 50% reduction is equivalent to what could be described as a heterozygous individual and would rarely generate a dominant phenotype. Likewise, the 12.5-mg/kg dosage facilitated the restoration levels of Mbnl1. This strategy could be a tact form of combatting DM1 by fine tuning the expression of MBNL1 without directly disturbing the endogenous expression of *DMPK* or *MBNL1*.

Another advantage of the antagomiR-23b was its notable long-term effects and low toxicity. One of the most pressing issues in antisense oligonucleotide therapy, along with off-target effects, is the delivery to the muscle. However, we see a significant improvement in the physical mouse muscle in this experiment. There are precedents in the literature that affirm that anti-miRs with a cholesterol group, known as antagomiRs, are able to reach muscle, among other tissues, very well;[43] therefore, we could say that we have managed to overcome this problem in mice despite the fact that exogenous administration of a chemically modified oligonucleotide can activate the body's natural immune response.[44] Additionally, the antagomiR has shown stability *in vivo* by its noted effects long term. Finally, the lack of toxic biochemistry profiles bodes well for the advancement of this particular chemistry.

miR-23b has been involved in several important developmental and cancer-related processes, in which it can either block tumorigenesis or enhance metastatic properties of cells depending on the biological context.[45] Indeed, loss of function of miR-23b has shown an increase of metastasis and tumor growth pathways in breast[46] and gastrointestinal[47] cancers. Conversely, miR-23b has also been shown to promote proliferation in ovarian and prostate cancer through the downregulation of its target phosphatase and tensin homolog (PTEN), which is a known tumor suppressor.[48,49] Whereas potential oncogenic effects cannot be assessed from 45 days of treatment, the association of miR-23b with the immune response can be partially addressed in our data. Specifically, neither the dose-response nor the time-response experiments provided any indication of proinflammatory activity, as indicated by healthy visual spleen size and monocyte counts in blood tests. It is true that decreasing miR-23b has been related to a strong increase in immune response[50] and that high doses of antisense drugs administered in a short period of time give rise to an acute response that causes the spleen to double in size.[51] Therefore, it should be noted that after 4 days with the antagomiR-23b and at the 40-mg/kg dose where miR-23b levels are practically nonexistent, no change in the spleen was visually observed. Taken together, low toxicity, high efficacy, and long-lasting biological effects at the molecular and functional levels highlight antagomiRs against miR-23b as a promising therapeutic strategy.

MATERIALS AND METHODS

Transgenic Mice and AntagomiR Administration

Mouse handling and experimental procedures conformed to the European law regarding laboratory animal care and experimentation (2003/65/CE) and were approved by Conselleria de Agricultura, Generalitat Valenciana (reference numbers A1529567788818 and A1458832800370). Homozygous transgenic HSA[LR] (line 20 b) mice[52] were provided by Prof. C. Thornton (University of Rochester Medical Center, Rochester, NY, USA) and mice with the corresponding genetic background (FVB) were used as controls. AntagomiR against miR-23b and the SC control was purchased from Creative Biogene. The modified sequence and the preparation of the oligo for subcutaneous injections were performed as previously described.[36] For intravenous injections, antagomiRs were reconstituted in PBS (KH$_2$PO$_4$ 0.144 g/L, NaCl 9 g/L, Na$_2$HPO$_4$ 0.795 g/L) at an adequate concentration to allow injection of the required

amount in only 100 μL. There are two PBS controls: one referring to the control used for 12.5 mg/kg in previous experiments[36] and another PBS for the 3-mg/kg and 40-mg/kg treatment concentrations. New mice injected with PBS have been introduced for the dose-response assay, because the mice used for this new assay are 1 month older than those previously injected at the dose of 12.5 mg/kg. The age of all of the mice used in this article ranges from 4.5 to 5.5 months, and mice were of the male sex.

RNA Extraction, RT-PCR, and qRT-PCR

Total RNA from murine GT and QD muscle was isolated using the miRNeasy Mini Kit (QIAGEN, Valencia, CA, USA), according to the manufacturer's instructions. 1 μg of RNA was digested with DNase I (Invitrogen) and reverse transcribed with SuperScript II (Invitrogen) using random hexanucleotides. For subsequent PCR reactions, 20 ng of cDNA was used with the GoTaq polymerase (Promega). Specific primers were used to analyze the alternative splicing of *Nfix* and *Clcn1* in mouse samples (QD and GT). *Gapdh* was used as the endogenous control using 0.2 ng of cDNA. PCR products were separated on a 2% agarose gel and quantified using ImageJ software (NIH). Percentage splice recovery (PSR) index was defined as value$\%_{SI}$ minus $\overline{X}\%_{DSI}$, divided by $\overline{X}\%_{DSI}$ minus $\overline{X}\%_{HSI}$ (where SI is splicing inclusion of each sample, DSI is disease splicing inclusion, and HSI is healthy splicing inclusion). This ratio was calculated for *Nfix* and *Clcn1*. The primer sequences and exons analyzed are available in Cerro-Herreros et al.[36] We used 1 ng of mouse tissue cDNA as a template for multiplex qRT-PCR using the QuantiFast Probe PCR Kit reagent. Commercial TaqMan probes (QIAGEN) were used for mouse (*Mbnl1*; 6-carboxyfluorescein [FAM]-labeled probes) and reference (*Gapdh*; NHS ester fluorophore [MAX]-labeled probe) genes. HSA transgene expression levels were determined by qRT-PCR, as described previously.[53] Mouse results were normalized to *Gapdh* endogenous gene expression.

miRNA expression in muscle tissues was quantified using specific miRCURY-locked nucleic acid miRNA PCR primers (Exiqon), according to the manufacturer's instructions. Relative gene expression was normalized to U1 and U6 small nuclear RNAs (snRNAs).

Expression levels were measured using an Applied Biosystems Quant-Studio 5 Real-Time PCR System. Expression relative to the endogenous gene and control group was calculated using the $2^{-\Delta\Delta Ct}$ method. Pairs of samples were compared using two-tailed t tests ($\alpha = 0.05$), applying Welch's correction when necessary.

ELISA

Mbnl1 protein was quantified by ELISA, according to the manufacturer's instructions (MyBioSource), in GT and QD muscles from HSA^{LR} mice. Briefly, 20–40 mg of muscle was homogenized in 200 μL of 1× PBS buffer (8 mM Na_2HPO_4, 150 mM NaCl, 2 mM KH_2PO_4, 3 mM KCl). All muscles used for the ELISA assay were processed at the same time using the same aliquot of PBS for all samples. Mbnl1 levels were expressed as nanogram of Mbnl1/mg of total pro-

tein. Total proteins were quantified with a bicinchoninic acid (BCA) protein assay kit (Pierce) using bovine serum albumin as a standard concentration range. The values were determined using a Tecan Infinite M200 PRO plate reader (Life Sciences).

Western Blotting

As confirmation of the results of ELISA, we performed a western blotting assay with sample pools. Each pool contained the protein extracted from samples of the same treatment. For total protein extraction, mouse muscles (GT and QD) were homogenized in radioimmunoprecipitation assay buffer (RIPA) buffer (150 mM NaCl, 1.0% IGEPAL, 0.5% sodium deoxycholate, 0.1% SDS, 50 mM Tris-HCl, pH 8.0), supplemented with protease and phosphatase inhibitor cocktails (Roche Applied Science). Total proteins were quantified with a BCA protein assay kit (Pierce) using bovine serum albumin as a standard concentration range. For the western blot assay, 20 μg of samples was denatured for 5 min at 100°C, electrophoresed on 12% SDS-PAGE gels, transferred onto 0.45 μm nitrocellulose membranes (GE Healthcare), and blocked with 5% nonfat dried milk in PBS-Tween 20 (PBS-T; 8 mM Na_2HPO_4, 150 mM NaCl, 2 mM KH_2PO_4, 3 mM KCl, 0.05% Tween 20, pH 7.4). Membranes were incubated overnight (O/N) at 4°C with primary mouse anti-MB1a (1:200, 4A8; Developmental Studies Hybridoma Bank) antibody. The anti-MBNL1 antibody was detected using horseradish peroxidase (HRP)-conjugated anti-mouse-immunoglobulin G (IgG) secondary antibody (1 h, 1:3,500; Sigma-Aldrich).

We determined the existence of the nuclear protein fraction in the muscle samples extracted with PBS. To do this, we loaded 20 μg of the protein onto polyacrylamide gels for SDS-PAGE. We transferred proteins to nitrocellulose membranes and carried out immunoblotting using anti-histone H3 (O/N; Millipore; 05-928, 1:1,000), followed by incubation with the appropriate secondary HRP-conjugated anti-rabbit-IgG secondary antibody (1 h, 1:3,500; Sigma-Aldrich). We diluted both antibodies in PBS containing 3% bovine serum albumin and 0.1% Tween 20.

Anti-GAPDH antibody (1 h, 1:3,500, clone G-9; Santa Cruz) was used as a loading control for mouse samples, followed by HRP-conjugated anti-mouse-IgG secondary antibody (1 h, 1:5,000; Sigma-Aldrich). Immunoreactive bands were detected using an enhanced chemiluminescence (ECL) Western Blotting Substrate (Pierce), and images were acquired with an ImageQuant LAS 4000 (GE Healthcare). Quantification was performed using ImageJ software (NIH).

Fluorescent Methods

In situ detection and Mbnl1 IF were performed as previously described.[54] Briefly, for foci detection, 10 mm frozen sections of the QD muscles were fixed in 3% paraformaldehyde (PFA)/PBS for 15 min at room temperature, washed with 1× PBS, and permeabilized with 0.5% Triton X-100/PBS for 5 min at room temperature. Fixed sections were incubated in the prehybridization buffer (2× saline sodium citrate [SSC], 30% deionized formamide) for 10 min at room

temperature and hybridized with a Cy3-(CAG)7-Cy3-labeled probe, diluted 1:200 in hybridization buffer, 30% formamide, for 2 h at 37°C in the dark. After hybridization, we washed the muscle sections with a prehybridization buffer for 30 min at 42°C, washed twice with 1 × SSC for 15 min at room temperature, washed with 1 × PBS, incubated with fluorescein isothiocyanate (FITC)-labeled wheat germ agglutinin diluted 1:600 in PBS for 45 min at room temperature to stain cell membranes, washed with PBS, and mounted with 4′,6-diamidino-2-phenylindole (DAPI) mounting media (Vector). A total of eight images per mice were taken using the LSM800 confocal microscope (Zeiss, Jena, Germany) at 400× magnification. To find the percentage of RNA nuclear foci, each image was quantified using the following formula:

$$\% \ nuclear \ Foci \ = \frac{Nuclei \ with \ foci}{Total \ nuclei} \times 100$$

Localization of Mbnl1 by IF was carried out with 10 mm frozen sections of QD muscles, fixed in 3% PFA/PBS for 15 min, washed with PBS, permeabilized with 0.5% Triton X-100/PBS for 5 min, and blocked in 5% normal goat serum in PBS for 30 min, all at room temperature. Sections were incubated O/N at 4°C with primary mouse anti-MBNL1 (1:200 clone MB1a; The Wolfson Centre for Inherited Neuromuscular Disease; in blocking buffer), washed with PBS, incubated with the secondary antibody (goat anti-mouse-FITC labeled, 1:200 in blocking buffer) in the dark for 1 h at room temperature, washed with PBS, and mounted with DAPI mounting media (Vector). A total of eight images for mice were taken using LSM800 confocal microscope (Zeiss, Jena, Germany) at 400× magnification. The Mbnl1 signal was quantified, dividing green channel intensity by the muscle area. ImageJ software measures intensity and pixel-size area from the confocal images.

Electromyography Studies
Electromyography was performed before the treatment, at the halfway point, and at the time of sacrifice under general anesthesia, as previously described.[23] Briefly, five needle insertions were performed in each QD muscle of both hind limbs, and myotonic discharges were graded on a five-point scale: 0, no myotonia; 1, occasional myotonic discharge in ≤50% of the needle insertions; 2, myotonic discharge in >50% of the insertions; 3, myotonic discharge in nearly all of the insertions; and 4, myotonic discharge in all insertions. The experiment was performed blindly to eliminate bias.

Forelimb Grip-Strength Test
The forelimb grip strength was measured with a Grip Strength Meter (BIO-GS3; Bioseb, USA). The peak pull force (measured in grams) was recorded on a digital force transducer when the mouse grasped the bar. The gauge of the force transducer was reset to 0 g after each measurement. The tension was recorded by the gauge at the time the mouse released its forepaws from the bar. We performed three consecutive measurements at 30-s intervals. The bodyweight measurement was performed in parallel. The experiment was performed blindly to eliminate bias.

The values of force are represented as the PNF, and it measures how close the weight-normalized strength values of treated HSA[LR] mice are compared to force measured in FVB controls. This PNF index is obtained by normalizing the weight-relative force (WRF; =force/weight) of each mouse after treatment with its WRF before initiating the treatment and dividing this value for the force effect (FE), resulting from dividing the mean WRF of FVB mice between the mean WRF of HSA[LR] treated with PBS at the same time point (PNF = WRF/FE).

Blood Assays
4, 15, 30, and 45 days following treatment, animals were sacrificed, and blood was collected by cardiac puncture exsanguination with K3-EDTA (SARSTEDT). The samples were analyzed by Laboratorios Montoro Botella (Valencia, Spain). White blood cell differential count (monocytes, stab cells, segmented cells, basophils, eosinophils, and lymphocytes) was measured with the Hematology Cell Counter AD-VIA 120 (Siemens). The serum biochemistry profile (creatinine, urea, amylase, alkaline phosphatase, ALT, bilirubin, lipase, and bile acids) was analyzed with the cobas 600 CCE modular analyzer (Roche).

Statistical Analyses
In the molecular and functional studies, for comparison on mean data, we assumed that all parameters follow a normal distribution, and the samples were compared using two-tailed t-tests ($\alpha = 0.05$), applying Welch's correction when necessary. The statistical differences were estimated by the Student's t-tests ($p < 0.05$) on normalized data. Sample size (n) can be seen in each figure. The graphs were generated using GraphPad Prism 6 software. The individual data for each mouse for the qPCR, ELISA, myotonia, force, splicing, Mbnl1, and foci IF can be found in Table S2.

Average values of blood parameters were compared by means of multivariate analysis of variance of compositional data using PBS-treated HSA[LR] mice as a reference. This is done by transforming the white blood cell differential count parameters as a set of elements from a simplex under Aitchison geometry,[55] applying ILR (isometric log ratio) transformation to the compositional data, and conducting a multivariate analysis of variance (MANOVA). Statistical analysis of the serum biochemistry profile was performed with a one-way ANOVA test or Kruskal-Wallis when application requirements did not hold for general linear modeling. In the cases in which the Kruskal-Wallis test gave a value lower than 0.05, a pairwise Wilcoxon rank sum test was performed with a p value correction for false discovery rate in order to see which of the treatments had different values from the rest. In all cases, all experiments (route, doses, or time) were analyzed together since it was not possible to analyze each group separately because there was no PBS control for each dose. Here, treatment type was also considered as the only independent factor using PBS-treated HSA[LR] mice as a reference.

The cutoff for statistical significance was set as $\alpha = 0.05$. Compositional data were analyzed with R package "compositions,"[56] whereas the serum biochemistry profile was analyzed with "R base."[57]

SUPPLEMENTAL INFORMATION

AUTHOR CONTRIBUTIONS

E.C.-H., M.P.-A., B.L., and R.A. designed the experiments. E.C.-H., I.G.-M., and N.M.-C. conducted all experiments. S.O. wrote the paper.

CONFLICTS OF INTEREST

B.L. is CEO and cofounder of Arthex Biotech. R.A. is advisor and cofounder of Arthex Biotech. The remaining authors declare no competing interests.

ACKNOWLEDGMENTS

REFERENCES

1. Landfeldt, E., Nikolenko, N., Jimenez-Moreno, C., Cumming, S., Monckton, D.G., Gorman, G., Turner, C., and Lochmüller, H. (2019). Disease burden of myotonic dystrophy type 1. J. Neurol. 266, 998–1006.

2. Mankodi, A., Teng-Umnuay, P., Krym, M., Henderson, D., Swanson, M., and Thornton, C.A. (2003). Ribonuclear inclusions in skeletal muscle in myotonic dystrophy types 1 and 2. Ann. Neurol. 54, 760–768.

3. Miller, J.W., Urbinati, C.R., Teng-Umnuay, P., Stenberg, M.G., Byrne, B.J., Thornton, C.A., and Swanson, M.S. (2000). Recruitment of human muscleblind proteins to (CUG)(n) expansions associated with myotonic dystrophy. EMBO J. 19, 4439–4448.

4. Sznajder, L.J., and Swanson, M.S. (2019). Short Tandem Repeat Expansions and RNA-Mediated Pathogenesis in Myotonic Dystrophy. Int. J. Mol. Sci. 20, 3365.

5. Konieczny, P., Stepniak-Konieczna, E., and Sobczak, K. (2014). MBNL proteins and their target RNAs, interaction and splicing regulation. Nucleic Acids Res. 42, 10873–10887.

6. Batra, R., Manchanda, M., and Swanson, M.S. (2015). Global insights into alternative polyadenylation regulation. RNA Biol. 12, 597–602.

7. Lin, X., Miller, J.W., Mankodi, A., Kanadia, R.N., Yuan, Y., Moxley, R.T., Swanson, M.S., and Thornton, C.A. (2006). Failure of MBNL1-dependent post-natal splicing transitions in myotonic dystrophy. Hum. Mol. Genet. 15, 2087–2097.

8. Wang, E.T., Ward, A.J., Cherone, J.M., Giudice, J., Wang, T.T., Treacy, D.J., Lambert, N.J., Freese, P., Saxena, T., Cooper, T.A., and Burge, C.B. (2015). Antagonistic regulation of mRNA expression and splicing by CELF and MBNL proteins. Genome Res. 25, 858–871.

9. Philips, A.V., Timchenko, L.T., and Cooper, T.A. (1998). Disruption of splicing regulated by a CUG-binding protein in myotonic dystrophy. Science 280, 737–741.

10. Ho, T.H., Charlet-B, N., Poulos, M.G., Singh, G., Swanson, M.S., and Cooper, T.A. (2004). Muscleblind proteins regulate alternative splicing. EMBO J. 23, 3103–3112.

11. Freyermuth, F., Rau, F., Kokunai, Y., Linke, T., Sellier, C., Nakamori, M., Kino, Y., Arandel, L., Jollet, A., Thibault, C., et al. (2016). Splicing misregulation of SCN5A contributes to cardiac-conduction delay and heart arrhythmia in myotonic dystrophy. Nat. Commun. 7, 11067.

12. Wheeler, T.M., Lueck, J.D., Swanson, M.S., Dirksen, R.T., and Thornton, C.A. (2007). Correction of ClC-1 splicing eliminates chloride channelopathy and myotonia in mouse models of myotonic dystrophy. J. Clin. Invest. 117, 3952–3957.

13. Fugier, C., Klein, A.F., Hammer, C., Vassilopoulos, S., Ivarsson, Y., Toussaint, A., Tosch, V., Vignaud, A., Ferry, A., Messaddeq, N., et al. (2011). Misregulated alternative splicing of BIN1 is associated with T tubule alterations and muscle weakness in myotonic dystrophy. Nat. Med. 17, 720–725.

14. Rau, F., Lainé, J., Ramanoudjame, L., Ferry, A., Arandel, L., Delalande, O., Jollet, A., Dingli, F., Lee, K.Y., Peccate, C., et al. (2015). Abnormal splicing switch of DMD's penultimate exon compromises muscle fibre maintenance in myotonic dystrophy. Nat. Commun. 6, 7205.

15. Batra, R., Charizanis, K., Manchanda, M., Mohan, A., Li, M., Finn, D.J., Goodwin, M., Zhang, C., Sobczak, K., Thornton, C.A., and Swanson, M.S. (2014). Loss of MBNL leads to disruption of developmentally regulated alternative polyadenylation in RNA-mediated disease. Mol. Cell 56, 311–322.

16. Masuda, A., Andersen, H.S., Doktor, T.K., Okamoto, T., Ito, M., Andresen, B.S., and Ohno, K. (2012). CUGBP1 and MBNL1 preferentially bind to 3′ UTRs and facilitate mRNA decay. Sci. Rep. 2, 209.

17. Rau, F., Freyermuth, F., Fugier, C., Villemin, J.P., Fischer, M.C., Jost, B., Dembele, D., Gourdon, G., Nicole, A., Duboc, D., et al. (2011). Misregulation of miR-1 processing is associated with heart defects in myotonic dystrophy. Nat. Struct. Mol. Biol. 18, 840–845.

18. Wang, E.T., Cody, N.A., Jog, S., Biancolella, M., Wang, T.T., Treacy, D.J., Luo, S., Schroth, G.P., Housman, D.E., Reddy, S., et al. (2012). Transcriptome-wide regulation of pre-mRNA splicing and mRNA localization by muscleblind proteins. Cell 150, 710–724.

19. Kanadia, R.N., Johnstone, K.A., Mankodi, A., Lungu, C., Thornton, C.A., Esson, D., Timmers, A.M., Hauswirth, W.W., and Swanson, M.S. (2003). A muscleblind knockout model for myotonic dystrophy. Science 302, 1978–1980.

20. Lee, K.Y., Li, M., Manchanda, M., Batra, R., Charizanis, K., Mohan, A., Warren, S.A., Chamberlain, C.M., Finn, D., Hong, H., et al. (2013). Compound loss of muscleblind-like function in myotonic dystrophy. EMBO Mol. Med. 5, 1887–1900.

21. Dixon, D.M., Choi, J., El-Ghazali, A., Park, S.Y., Roos, K.P., Jordan, M.C., Fishbein, M.C., Comai, L., and Reddy, S. (2015). Loss of muscleblind-like 1 results in cardiac pathology and persistence of embryonic splice isoforms. Sci. Rep. 5, 9042.

22. Osborne, R.J., Lin, X., Welle, S., Sobczak, K., O'Rourke, J.R., Swanson, M.S., and Thornton, C.A. (2009). Transcriptional and post-transcriptional impact of toxic RNA in myotonic dystrophy. Hum. Mol. Genet. 18, 1471–1481.

23. Kanadia, R.N., Shin, J., Yuan, Y., Beattie, S.G., Wheeler, T.M., Thornton, C.A., and Swanson, M.S. (2006). Reversal of RNA missplicing and myotonia after muscleblind overexpression in a mouse poly(CUG) model for myotonic dystrophy. Proc. Natl. Acad. Sci. USA 103, 11748–11753.

24. Chakraborty, M., Sellier, C., Ney, M., Pascal, V., Charlet-Berguerand, N., Artero, R., and Llamusi, B. (2018). Daunorubicin reduces MBNL1 sequestration caused by CUG-repeat expansion and rescues cardiac dysfunctions in a Drosophila model of myotonic dystrophy. Dis. Model. Mech. 11, dmm032557.

25. Chakraborty, M., Selma-Soriano, E., Magny, E., Couso, J.P., Pérez-Alonso, M., Charlet-Berguerand, N., Artero, R., and Llamusi, B. (2015). Pentamidine rescues contractility and rhythmicity in a Drosophila model of myotonic dystrophy heart dysfunction. Dis. Model. Mech. 8, 1569–1578.

26. de Haro, M., Al-Ramahi, I., De Gouyon, B., Ukani, L., Rosa, A., Faustino, N.A., Ashizawa, T., Cooper, T.A., and Botas, J. (2006). MBNL1 and CUGBP1 modify expanded CUG-induced toxicity in a Drosophila model of myotonic dystrophy type 1. Hum. Mol. Genet. 15, 2138–2145.

27. Bargiela, A., Cerro-Herreros, E., Fernandez-Costa, J.M., Vilchez, J.J., Llamusi, B., and Artero, R. (2015). Increased autophagy and apoptosis contribute to muscle atrophy in a myotonic dystrophy type 1 Drosophila model. Dis. Model. Mech. 8, 679–690.

28. Bargiela, A., Sabater-Arcis, M., Espinosa-Espinosa, J., Zulaica, M., Lopez de Munain, A., and Artero, R. (2019). Increased Muscleblind levels by chloroquine treatment improve myotonic dystrophy type 1 phenotypes in in vitro and in vivo models. Proc. Natl. Acad. Sci. USA 116, 25203–25213.

29. Chamberlain, C.M., and Ranum, L.P. (2012). Mouse model of muscleblind-like 1 overexpression: skeletal muscle effects and therapeutic promise. Hum. Mol. Genet. 21, 4645–4654.

30. Chen, G., Masuda, A., Konishi, H., Ohkawara, B., Ito, M., Kinoshita, M., Kiyama, H., Matsuura, T., and Ohno, K. (2016). Phenylbutazone induces expression of MBNL1 and suppresses formation of MBNL1-CUG RNA foci in a mouse model of myotonic dystrophy. Sci. Rep. 6, 25317.

31. Zhang, F., Bodycombe, N.E., Haskell, K.M., Sun, Y.L., Wang, E.T., Morris, C.A., Jones, L.H., Wood, L.D., and Pletcher, M.T. (2017). A flow cytometry-based screen identifies MBNL1 modulators that rescue splicing defects in myotonic dystrophy type I. Hum. Mol. Genet. 26, 3056–3068.

32. Huin, V., Vasseur, F., Schraen-Maschke, S., Dhaenens, C.M., Devos, P., Dupont, K., Sergeant, N., Buée, L., Lacour, A., Hofmann-Radvanyi, H., and Sablonnière, B. (2013). MBNL1 gene variants as modifiers of disease severity in myotonic dystrophy type 1. J. Neurol. 260, 998–1003.

33. Bartel, D.P. (2018). Metazoan MicroRNAs. Cell 173, 20–51.

34. López Castel, A., Overby, S.J., and Artero, R. (2019). MicroRNA-Based Therapeutic Perspectives in Myotonic Dystrophy. Int. J. Mol. Sci. 20, 5600.

35. Cerro-Herreros, E., Fernandez-Costa, J.M., Sabater-Arcis, M., Llamusi, B., and Artero, R. (2016). Derepressing muscleblind expression by miRNA sponges ameliorates myotonic dystrophy-like phenotypes in Drosophila. Sci. Rep. 6, 36230.

36. Cerro-Herreros, E., Sabater-Arcis, M., Fernandez-Costa, J.M., Moreno, N., Perez-Alonso, M., Llamusi, B., and Artero, R. (2018). miR-23b and miR-218 silencing increase Muscleblind-like expression and alleviate myotonic dystrophy phenotypes in mammalian models. Nat. Commun. 9, 2482.

37. Shen, W., De Hoyos, C.L., Migawa, M.T., Vickers, T.A., Sun, H., Low, A., Bell, T.A., 3rd, Rahdar, M., Mukhopadhyay, S., Hart, C.E., et al. (2019). Chemical modification of PS-ASO therapeutics reduces cellular protein-binding and improves the therapeutic index. Nat. Biotechnol. 37, 640–650.

38. Pettersson, O.J., Aagaard, L., Jensen, T.G., and Damgaard, C.K. (2015). Molecular mechanisms in DM1 - a focus on foci. Nucleic Acids Res. 43, 2433–2441.

39. Tinsley, J., Robinson, N., and Davies, K.E. (2015). Safety, tolerability, and pharmacokinetics of SMT C1100, a 2-arylbenzoxazole utrophin modulator, following single- and multiple-dose administration to healthy male adult volunteers. J. Clin. Pharmacol. 55, 698–707.

40. Kulkarni, M., Ozgur, S., and Stoecklin, G. (2010). On track with P-bodies. Biochem. Soc. Trans. 38, 242–251.

41. Neriec, N., and Percipalle, P. (2018). Sorting mRNA Molecules for Cytoplasmic Transport and Localization. Front. Genet. 9, 510.

42. Adereth, Y., Dammai, V., Kose, N., Li, R., and Hsu, T. (2005). RNA-dependent integrin alpha3 protein localization regulated by the Muscleblind-like protein MLP1. Nat. Cell Biol. 7, 1240–1247.

43. Krützfeldt, J., Rajewsky, N., Braich, R., Rajeev, K.G., Tuschl, T., Manoharan, M., and Stoffel, M. (2005). Silencing of microRNAs in vivo with 'antagomirs'. Nature 438, 685–689.

44. Shen, X., and Corey, D.R. (2018). Chemistry, mechanism and clinical status of antisense oligonucleotides and duplex RNAs. Nucleic Acids Res. 46, 1584–1600.

45. Wang, W., Wang, Y., Liu, W., and van Wijnen, A.J. (2018). Regulation and biological roles of the multifaceted miRNA-23b (MIR23B). Gene 642, 103–109.

46. Pellegrino, L., Stebbing, J., Braga, V.M., Frampton, A.E., Jacob, J., Buluwela, L., Jiao, L.R., Periyasamy, M., Madsen, C.D., Caley, M.P., et al. (2013). miR-23b regulates cytoskeletal remodeling, motility and metastasis by directly targeting multiple transcripts. Nucleic Acids Res. 41, 5400–5412.

47. Zhang, H., Hao, Y., Yang, J., Zhou, Y., Li, J., Yin, S., Sun, C., Ma, M., Huang, Y., and Xi, J.J. (2011). Genome-wide functional screening of miR-23b as a pleiotropic modulator suppressing cancer metastasis. Nat. Commun. 2, 554.

48. Tian, L., Fang, Y.X., Xue, J.L., and Chen, J.Z. (2013). Four microRNAs promote prostate cell proliferation with regulation of PTEN and its downstream signals in vitro. PLoS ONE 8, e75885.

49. Vaksman, O., Tropé, C., Davidson, B., and Reich, R. (2014). Exosome-derived miRNAs and ovarian carcinoma progression. Carcinogenesis 35, 2113–2120.

50. Zhu, S., Pan, W., Song, X., Liu, Y., Shao, X., Tang, Y., Liang, D., He, D., Wang, H., Liu, W., et al. (2012). The microRNA miR-23b suppresses IL-17-associated autoimmune inflammation by targeting TAB2, TAB3 and IKK-α. Nat. Med. 18, 1077–1086.

51. Kamola, P.J., Maratou, K., Wilson, P.A., Rush, K., Mullaney, T., McKevitt, T., Evans, P., Ridings, J., Chowdhury, P., Roulois, A., et al. (2017). Strategies for In Vivo Screening and Mitigation of Hepatotoxicity Associated with Antisense Drugs. Mol. Ther. Nucleic Acids 8, 383–394.

52. Mankodi, A., Logigian, E., Callahan, L., McClain, C., White, R., Henderson, D., Krym, M., and Thornton, C.A. (2000). Myotonic dystrophy in transgenic mice expressing an expanded CUG repeat. Science 289, 1769–1773.

53. Wheeler, T.M., Sobczak, K., Lueck, J.D., Osborne, R.J., Lin, X., Dirksen, R.T., and Thornton, C.A. (2009). Reversal of RNA dominance by displacement of protein sequestered on triplet repeat RNA. Science 325, 336–339.

54. Bisset, D.R., Stepniak-Konieczna, E.A., Zavaljevski, M., Wei, J., Carter, G.T., Weiss, M.D., and Chamberlain, J.R. (2015). Therapeutic impact of systemic AAV-mediated RNA interference in a mouse model of myotonic dystrophy. Hum. Mol. Genet. 24, 4971–4983.

55. Aitchison, J., Barceló-Vidal, C., Egozcue, J.J., and Pawlowsky-Glahn, V. (2002). A concise guide for the algebraic-geometric structure of the simplex, the sample space for compositional data analysis. In Proceedings of IAMG'02—the VIII Annual Conference of the International Association for Mathematical Geology, Vol I and II, U. Bayer, H. Burger, and W. Skala, eds (Selbstverlag der Alfred-Wegener-Stiftung), pp. 387–392.

56. van den Boogaart, K.G., Tolosana-Delgado, R., and Bren, M. (2018). Compositions: compositional data analysis (R package). R (version 1.40-2).

57. R Development Core Team (2019). R: A language and environment for statistical computing (R Foundation for Statistical Computing).